HHS Public Access

Author manuscript

IEEE Trans Biomed Eng. Author manuscript; available in PMC 2023 December 01.

Published in final edited form as:

IEEE Trans Biomed Eng. 2022 December ; 69(12): 3582–3590. doi:10.1109/TBME.2022.3172429.

The Unique Magnetic Signature of Sickle Red Blood Cells: A Comparison Between the Red Blood Cells of Transfused and Non-Transfused Sickle Cell Disease Patients and Healthy Donors

Mitchell Weigand[#],
Ohio State University, Columbus, OH, USA.

Jenifer Gómez-Pastora[#],
The Ohio State University and is now with Texas Tech University, Lubbock, TX, USA.

Jacob Strayer[#],
Ohio State University, Columbus, OH, USA.

Xian Wu,
Ohio State University, Columbus, OH, USA.

Hyeon Choe,
Ohio State University, Columbus, OH, USA.

Shuwei Lu,
Ohio State University, Columbus, OH, USA.

Eric Plencner,
Ohio State University, Columbus, OH, USA.

Kristina Landes,
Ohio State University, Columbus, OH, USA.

Andre Palmer,
Ohio State University, Columbus, OH, USA.

Maciej Zborowski,
Cleveland Clinic, Cleveland, OH, USA.

Payal Desai,
Ohio State University, Columbus, OH, USA.

Jeffrey Chalmers
Ohio State University, Columbus, OH, USA.

[#] These authors contributed equally to this work.

Abstract

Sickle cell disease (SCD) is an inherited blood disorder that affects millions of people worldwide, especially in low–resource regions of the world, where a rapid and affordable test to properly

(correspondence Weigand.49@osu.edu).

diagnose the disease would be highly valued. Magnetophoresis is a technique that could simultaneously analyze, quantify, and potentially separate the patient's sickle red blood cells (RBCs) from healthy RBCs, but the magnetic characteristics of sickle RBCs have yet to be reported. In this work, we present the single cell magnetic characterization of RBCs obtained from SCD patients. Sufficient single cells are analyzed from patient samples undergoing transfusion therapy and not yet having transfusion therapy (TP and NTP, respectively), such that means and distributions of these single RBC mobilities are created in the form of histograms which facilitated comparison to RBCs from healthy donors (HD). The magnetic characterization is obtained using a technique known as Cell Tracking Velocimetry (CTV) that quantitatively characterizes the RBC response to magnetic and gravitational fields. The magnetic properties of RBCs containing oxygenated, deoxygenated hemoglobin (Hb) and methemoglobin (oxyHb–RBCs, deoxyHb–RBCs, and metHb–RBCs) are further determined. The NTP samples report the highest magnetic character, especially when compared to oxyHb–RBCs from HD, which implies impaired oxygen binding capabilities. Also, the oxygen–Hb equilibrium curves are obtained to estimate the magnetic character of the cells under intermediate oxygen levels. Our results confirm higher magnetic moment of SCD blood (NTP) under intermediate oxygen levels. These data demonstrate the potential feasibility of magnetophoresis to identify, quantify and separate sickle RBCs from healthy RBCs.

Keywords

Sickle cell disease (SCD); magnetophoresis; single-cell analysis; anemia; cell tracking velocimetry (CTV); oxygen-Hb equilibrium; blood oxygen binding system

I. Introduction

Sickle cell disease (SCD) is an inherited blood disorder that affects millions of people worldwide; it affects 25% of people living in Central and West Africa and approximately 100,000 people in the United States, mostly of African descent [1−3] have the most serious form, the so called homozygous, HbSS, form of the disease. This hemoglobinopathy is the first described instance of a "molecular disease" and is caused by a single amino acid mutation in the β–globin gene of hemoglobin (Hb). Upon deoxygenation, sickle Hb (HbS) enters the tense (T) conformational state, where the mutant valine is able to induce polymerization of HbS, which is subsequently reported to dehydrate and shrivel the erythrocyte. This results in hardened and elongated red blood cells (RBCs) that do not uptake oxygen efficiently, obstruct blood vessels, and increase blood viscosity [4], In addition to the previously mentioned homozygous HbSS, other severe forms of SCD include compound heterozygous conditions, such as HbC with HbS (HbSC), HbS with β–thalassemia (HbS/β^0 − thalassemia or HbS/β+ − thalassemia), and HbS with other beta–globin variants such as HbSD or $HbSO^{Arab}$, all of which express sufficient HbS to cause intracellular sickling [2], The inheritance of both HbA and HbS (HbAS) corresponds to sickle cell trait; strictly not a form of SCD but that may be associated with adverse health outcomes [2], Although sickle cell trait affects between 1 and 3 million Americans, 8 to 10% of African Americans, and more than 100 million people worldwide, these patients rarely require treatment and blood from such donors is not considered in the present work [5].

The RBCs in a person without SCD circulate in the bloodstream for approximately 120 days and are replaced by new cells synthesized in the bone marrow; however, it is reported that sickle RBCs survive only 10 to 20 days in the circulation, resulting in hemolytic anemia characterized by a decrease in the number of circulating RBCs and total [Hb] [3], Sickle cells are stiff, distorted in shape and sometimes block small blood vessels, causing vaso-occlusive crises (VOCs). Individuals with SCD suffer a range of conditions, including acute anemia, infections, tissue and organ damage, severe pain, acute chest syndrome, and strokes [2]. The median life expectancy for those with SCD is 40 to 50 years [3]. Although gene therapy approaches have been successful, there is no widely used cure for SCD. In some cases, hydroxyurea is prescribed to increase the levels of Hb and fetal Hb (HbF) and to reduce the frequency of painful episodes [6]. Another common treatment is regular blood transfusions. However, the annual cost of transfusions rises to several thousand dollars per year, and although they are effective, they are financially inaccessible to the majority of SCD patients [7]. Moreover, they pose significant clinical challenges and transfusion-related complications exist, such as alloimmunization, delayed hemolytic transfusion reactions, and iron overload [8–10].

SCD is best managed when diagnosed early, but since SCD is most prevalent in low-resource regions of the world, screening for SCD is rare and diagnosis at the point-of-care (POC) is challenging. In fact, in many regions, most affected children die undiagnosed before the age of 5 years [11]. Many SCD diagnostic techniques exist; however, they either suffer from high costs and require trained operators such as blood smears (however morphology-based imaging classification algorithms are improving), HPLC, or electrophoresis (detects all mutations), and isoelectric focusing (the current standard test for newborns, and takes 45 minutes) or inaccuracy such as a chemical-induced turbidity test (cannot differentiate sickle cell trait/disease, inaccurate in newborns, coinheritance of other diseases, erythrocytosis and others). [12, 26, 47] After an initial diagnosis, however, there are no rapid tests to detect a VOC, although Ballas and Smith have report that changes in RBC density, deformability, reticulocyte count, and Hb levels often precede one [45]. Thus, a rapid and affordable tool that has the means to detect the hematological and physical properties accompanying a VOC is needed. There are additional methods in the research stages that involve image capture during induced sickling, elasticity and deformation measurement, rapid lateral flow assays, and centrifugation. [12] However, there are currently no tests that can detect a VOC.

A technique that could be used to simultaneously analyze, quantify, and potentially separate the patient’s sickle RBCs from healthy RBCs is magnetophoresis. The magnetic susceptibility of Hb depends on the oxidative state and oxygen binding of Hb’s four iron (Fe) atoms. The works of Pauling, Coryell, and others indicated that for deoxygenated ferrous Hb and for methemoglobin (the oxidized form of Hb), the presence of unpaired electrons when the Fe is attached to the surrounding protoporphyrin and histidine side chain by ionic bonds makes these species paramagnetic whereas oxygenated, ferrous Hb has no unpaired electrons due to its covalent bonds and is diamagnetic in nature [13–15]. The separation and analysis of RBCs from other cell types using magnetic means has been reported widely in the literature [16–20]. Moreover, magnetic devices (magnetic levitation devices, mostly) have been proposed for the diagnosis of SCD [21–25]. Nevertheless, the

potential of this technique to analyze, quantify and separate sickle RBCs from SCD patients is not yet clear, since information regarding the RBC properties of SCD patients at the single cell level is not available. Especially important is understanding the physicochemical properties of Hb and how they influence the magnetic behavior of RBCs (e.g., ability to bind oxygen), along with other properties that might affect the magnetic separation, such as the density, shape, and deformability of erythrocytes. It has been demonstrated that in SCD, the presence of sickle RBCs, characterized by cellular dehydration and polymerization of HbS, affects the volume, density, size, intracellular Hb concentration, and oxygen affinity of the RBC [26–29]. A recent study on bulk volume susceptibility difference between deoxyhemoglobin and oxyhemoglobin for HbS and HbA by blood-oxygen level dependent (BOLD) nuclear magnetic resonance imaging (MRI) reports no difference although, interestingly, that study shows greater spread of data for HbS than for HbA samples [30]. A comparative study using ab-initio quantum-mechanical simulations of the electronic structure of HbS and HbA's active centers reports no difference in the intensity of magnetization of the Fe atom in HbS and HbA molecules not bound to O_2 and a small excess of magnetization in the O_2-HbS complex compared to O_2-HbA complex [31]. A recent, detailed quantum-mechanical simulations study on the effective magnetization of Fe in the heme cluster points to a significant contribution of the neighboring atoms of the globin molecule [32], which could be affected by the Hb polymerization in the HbS molecule.

In this work, we report for the first time, single cell scale magnetic characterization of RBCs obtained from SCD patients both requiring and not requiring chronic transfusion therapy. The analysis is carried out by using different instruments. First, an instrument referred to as Cell Tracking Velocimetry (CTV) is employed, which has been previously used to characterize the magnetic behavior of individual cells or particles. Aside from permanent magnets, camera, light source and a computer, the only recurring costs come from the blood draw and isotonic buffer. Additionally, data sampling can yield several hundred datapoints in a few minutes of sampling [33–36]. More specifically, the CTV was used to evaluate the magnetic properties of individual RBCs containing either fully oxygenated Hb (oxyHb-RBCs), deoxygenated Hb (deoxyHb-RBCs) and methemoglobin (metHb-RBCs). Complementary to the CTV measurements, the oxygen-Hb equilibrium curves from these same samples are obtained by using a Blood Oxygen Binding System (BOBS). In addition to the oxygen-Hb equilibrium curves, estimates are made of the magnetic character of SCD samples under intermediate oxygen levels. The data obtained from SCD patient RBCs are also compared to the magnetic properties of RBCs obtained from healthy donors. Our results confirm a difference in the properties of the RBCs obtained from SCD patients and healthy donors, especially under intermediate oxygen saturation levels. Thus, this work might open the door to the possible detection, quantification, and magnetic separation of sickle cells from SCD patients.

II. Methods

A. Sample Preparation

A total of 15 RBC samples obtained from healthy individuals and SCD patients receiving and not receiving chronic transfusion therapy (at least for the last 3 months prior to sample collection) were collected following informed consent according to protocols approved by the Institutional Review Board (IRB) of The Ohio State University (protocol numbers 2021H0075 and 2018H0268; approved March 29th, 2021 and July 20th, 2018, respectively). All experiments were performed in accordance with relevant guidelines and regulations. For the healthy donor RBC samples (HD samples), approximately 5 mL of whole blood was drawn into a 10 mL collection tube containing EDTA anticoagulant. For the SCD patients not requiring transfusion therapy (NTP samples), the same protocol was observed, where 5 mL of whole blood was collected into 10 mL tubes containing EDTA anticoagulant. For SCD patients requiring transfusion therapy (TP samples), the discarded RBCs were collected in a bag containing citrate while the patient received RBC exchange apheresis. The samples (variable volumes of the discarded RBC) were taken directly from the apheresis collection bag after the exchange was complete.

The RBCs from HD and NTP whole blood and TP apheresis waste product were washed in phosphate buffered saline (PBS) using centrifugation (three times at 1300 x g for 5 mins), as presented in Fig. 1. After washing, the average density of RBCs was determined by centrifugation (1000 x g for 15 mins) using a Percoll gradient (Cytiva Sweden AB, Sweden) and density marker beads (Amersham Biosciences AB, Sweden), which are colored microspheres of known mass density that are used for determining the density of cells in gradient columns, as shown in Fig. 1. All samples were introduced into an automated cell counter, B23005 Multisizer 4e Coulter Counter (CC, Beckman Coulter, CA), to measure the cell concentration as well as volume (and equivalent diameter) distributions.

After preparing RBC samples and determining size and concentration distributions, RBCs were divided into three aliquots designated “oxyHb-RBCs,” “deoxyHb-RBCs,” and “metHb-RBCs” for CTV analysis. OxyHb-RBCs were exposed to room air for 10 min and mixed to ensure that the cells were in the oxyHb state. The paramagnetic forms of RBCs (deoxyHb-RBCs and metHb-RBCs) were obtained after treating the washed RBCs with sodium dithionite (deoxyHb-RBCs) (while avoiding mixing/stirring) and sodium nitrite (metHb-RBCs) as previously reported in the literature [34, 37]. The oxygenation state of the oxyHb-RBC and deoxyHb-RBC samples was ensured by measuring the pO_2 (partial pressure of oxygen, which reflects the amount of oxygen gas dissolved in the blood sample) using a blood gas analyzer (RAPIDLab 248, Siemens Healthcare Diagnostics, German) before CTV analysis. OxyHb-RBCs and deoxyHb-RBCs had pO_2 values around 180 and 0 mmHg, respectively. Finally, BOBS analyzed oxyHb-RBCs. In Fig. 1, the workflow of the sample preparation procedure is schematized.

B. Cell Tracking Velocimetry Analysis

Once the samples were prepared, the magnetic characterization of fully oxygenated, deoxygenated, and oxidized RBCs was performed using CTV. CTV uses a microscope,

camera, permanent NdFeB magnets and a microfluidic channel to track the movement of cells and particles under the direct influence of magnetic and gravitational fields. More specifically, CTV measures the magnetically induced velocity (u_m) and gravity induced settling velocity (u_s) of cells in a region of interest, where a high, uniform, and well characterized magnetic energy gradient (S_m), perpendicular to gravity, is created. Once the RBCs are injected, horizontal and vertical velocities are measured, which can be related to specific cellular and magnetic field properties. The magnetically and gravitationally induced velocities, u_m and u_s can be described as follows:

$$u_m = \frac{(\chi_{Cell} - \chi_{Fluid})V_{Cell}}{f_d 3\pi D_{Cell}\eta} S_m \tag{1}$$

$$u_s = \frac{(\rho_{Cell} - \rho_{Fluid})V_{Cell}}{f_d 3\pi D_{Cell}\eta} g \tag{2}$$

where the subscripts cell and fluid refer to the cell and the suspending fluid, χ is the magnetic susceptibility, ρ is the density, D and V are the diameter and volume of the RBC, η is the viscosity of the suspending fluid, f_d is the drag coefficient (1.0 for spheres and 1.23 for disc-shaped erythrocytes) and g is the acceleration due to gravity (9.8 m/s^2) [37]. S_m is defined by:

$$S_m = \frac{\left|VB^2\right|}{2\mu_0} \tag{3}$$

where μ_0 and B are the permeability of free space and the magnetic flux density at the RBC, respectively. Rearranging (1) and (2) leads to:

$$\chi_{Cell} = \chi_{Fluid} + \frac{u_m}{u_s}\frac{(\rho_{Cell} - \rho_{Fluid})g}{s_m} \tag{4}$$

The RBC magnetic susceptibility is the material property of its constituents and does not depend on the RBC size (volume and diameter) nor the fluid viscosity. Moreover, the relationship between the magnetic and settling velocity and the mass and concentration of Hb in the RBCs, the mean corpuscular Hb (MCH) and the mean corpuscular Hb concentration (MCHC), can be estimated as [17, 34]:

$$MCH = \frac{9 * 2^{0.5}\pi}{Sm * (\chi_{m,Hb} + \chi_{m,globin} - \chi_{H_2O}) * V_{Hb}} * \left[\frac{(f_d * u_m) * (f_d * u_s)^{0.5} * \eta^{1.5}}{\Delta\ \rho^{0.5} * g^{0.5}}\right] * 10^3 * MW_{Hb} \tag{5}$$

$$MCHC = \frac{\left(\frac{u_m}{u_S}\right)(\Delta\rho)\left(\frac{g}{S_m}\right)}{(\chi_{m,Hb} + \chi_{m,globin} - \chi_{H_2O}) * V_{Hb}} * MW_{Hb} \tag{6}$$

where $V_{Hb} = 48.23$ L/mol is the molar volume of Hb, MW_{Hb} is the molecular weight of Hb (64,450 g/mol), $\chi_{m,globin} = -37,830 \times 10^{-9}$ L/mol is the molar susceptibility of the globin chain, and $\chi_{H2O} = -12.97 \times 10^{-9}$ L/mol is the molar susceptibility of water. The molar susceptibility of the deoxygenated Hb heme group is $\chi_{m,deoxyHb} = 50,890 \times 10^{-9}$ L/mol, and that of the metHb heme group is $\chi_{m,metHb} = 56,000 \times 10^{-9}$ L/mol (all in CGS system of units). The molar susceptibility of the oxyHb heme group is zero.

After introducing the different RBC samples into the CTV, images of the cells' location were captured using an in-house program and analyzed using the TrackMate plugin on ImageJ [39] and in-house programs to calculate u_m and u_s. With these data, χ_{RBC} as well as the MCH and MCHC were calculated.

C. Blood Oxygen Binding System Measurements

Washed, oxyHb-RBCs were also analyzed in the BOBS (Loligo Systems, Viborg, Denmark). BOBS continuously performs UV-visible spectroscopy while passing a varying mixture of O_2/N_2 over a thin film of RBC sample. This allows the operator to determine the oxygen saturation of Hb (SO_2) as a function of oxygen partial pressure (pO_2) (i.e., the oxygen-Hb equilibrium curve). From this curve, the oxygen partial pressure at 50% saturation (P_{50}) is determined. The BOBS was operated at 37°C with a gas temperature offset of +1.3°C. Samples were prepared by diluting cells to a concentration of approximately 70 million cells/mL using Hemox buffer (TCS Scientific Corp, New Hope, PA) with 1% additive A, and 1% additive B (TCS Scientific) at 7.4 pH. The BOBS system was refilled with 20 mL deionized water prior to each experiment session. A 2 μL sample was spread onto the glass sample plate and allowed to acclimate to system temperature before start of the run. A gas mixing system was used to automatically mix O_2 and N_2 entering the BOBS and our protocol specified an incremental increase of O_2 from 0% to 22% (incremental value of 0.1–1%), while the Soret peak intensity was measured. Data obtained from the BOBS was standardized and fit to the Hill equation in an R (RStudio, Boston, MA) script to regress the P_{50} value and Hill coefficient (n) for cooperative oxygen binding to Hb [40]. More specifically, the oxygen-Hb equilibrium curve was fitted to the following equation used to describe cooperative binding to ligands:

$$S_{O_2} = \frac{pO_2^n}{P_{50}^n + pO_2^n} \tag{7}$$

Moreover, we used the Adair model to estimate the magnetic character of the samples under intermediate oxygenation states [41]. Hb is a tetrameric protein where each of the four globin subunits can bind a single oxygen molecule, as presented in the following equation:

$$O_2 + Hb(O_2)_{i-1} \leftrightarrow Hb(O_2)_i \tag{8}$$

where $1 \leq i \leq 4$.

Pauling determined that the magnetic moment of an unoccupied Hb subunit (i.e., not bound with oxygen) is 5.46 Bohr magnetons and when bound with oxygen is zero [14]. Recently, it has been experimentally demonstrated that the magnetic moment of healthy RBCs is inversely proportional to oxygen partial pressure [42]. In this work, we investigate the differences in the oxygen affinity among HD, TP and NTP samples, with the purpose of eventually exploiting these differences to develop a magnetophoretic device to diagnose SCD and to quantify the number or percentage of sickle RBCs in the blood of SCD patients, as well as to design a separator to isolate sickle from healthy RBCs. To calculate the magnetic moment of Hb and RBCs as a function of pO_2, the Adair model was fit to oxygen-Hb equilibrium data to determine the equilibrium constants (K_i), as follows [41]:

$$S_{O_2} = \frac{K_1[O_2] + 2\ K_1 K_2\{O_2\}^2 + 3\ K_1 K_2 K_3[O_2]^3 + 4\ K_1 K_2 K_3 K_4[O_2]^4}{4\left(1 + K_1[O_2] + 2\ K_1 K_2\{O_2\}^2 + 3\ K_1 K_2 K_3[O_2]^3 + 4\ K_1 K_2 K_3 K_4[O_2]^4\right)} \tag{9}$$

$$K_i = \frac{[Hb(O_2)_i]}{[Hb(O_2)_{i-1}][O_2]} \tag{10}$$

From the equilibrium constants K_i the mole fraction of intermediate oxygen-Hb species ($Hb(O2)_i$) can be quantitated ($XHb(O2)_i$) as a function of pO_2, and this allows the determination of the magnetic moment of the samples (M_{Hb}), as follows:

$$x_{Hb(O_2)i} = \frac{K_i[Hb(O_2)_{i-1}][O_2]}{[Hb] + \sum_{i=1}^{4} K_i[Hb(O_2)_{i-1}][O_2]} \tag{11}$$

$$M_{Hb} = 5.46 * \left(4 - \left(\sum_{i=1}^{4} i * x_{Hb(O_2)i}\right)\right) \tag{12}$$

III. Results and Discussion

In order to understand the differences between RBCs from SCD transfused (TP samples), non-transfused patients (NTP samples) and healthy donors (HD samples), five blood samples from each source were analyzed and several RBC parameters were collected. Table I reports the average (and standard deviation) for each sample. From the Coulter Counter, the red cell diameter was obtained. From CTV, several RBC indices such as MCH and MCHC were estimated after measuring the settling and magnetic velocities of deoxyHb-RBCs and metHb-RBCs. Finally, the P_{50} from BOBS is reported. These parameters and the different analyses performed are discussed in the following section below.

A. CTV Analysis

The raw data from the CTV instrument is the settling and magnetic velocities, from which the magnetic susceptibility of RBCs is determined and the MCH and MCHC RBC indices calculated. Table I reports the average values obtained from this analysis and Figs. 2 and

3 present the CTV trajectories (cell's velocities), grouped by donor type: ND, NTP, TP, respectively.

Fig. 2 presents the data in form of dot plots of u_s versus u_m, and the cumulative distribution curves as function of the specific velocity. Fig. 3 presents the data for each of the three states in the form of histograms, the donor samples within each of these states averaged.

The average u_m of oxyHb-RBCs is negative for all groups. This has been previously reported and is expected since oxyHb RBCs are not only diamagnetic, but the average magnitude of this property is less than the suspending buffer (PBS) [18]. In contrast, both the deoxyHb-RBCs and metHb-RBCs have positive u_m values, consistent with the paramagnetic property of deoxyHb and metHb. The u_m of deoxyHb-RBCs is slightly greater than metHb-RBCs, consistent with the small difference in mobility between these chemical states of Hb, as previously reported in the literature [15]. Although these measurable differences in mobility and sedimentation exist between different samples, there is a large degree of heterogeneity within samples, particularly those from SCD patients. Future studies that correlate common hematological parameters to this heterogeneity may reveal causes of this observation.

Inspection of the histograms in Fig. 3 indicated a noticeable "right shift" in the magnetic mobility of the NTP donor blood relative to the HD and TP samples. This is detectable in each of the three states: oxy, deoxy, and met. Further inspection suggests that, when comparing the settling velocity, deoxyHb-RBCs have a decreased u_s in TP (Fig. 3 c)) and NTP (Fig. 3 b)) samples. This suggests a decreased density, decreased size/volume, or increased drag due to a change in shape when the RBCs are treated with sodium dithionite compared to the same samples treated with sodium nitrite (metHb-RBCs). However, u_s data suggest that the density, size, and drag are unchanged in healthy RBCs when subjected to different chemical states, as presented in Fig. 3 a). However, care should be taken since the standard deviations are sufficiently high that these observations are only speculations.

The decrease in the u_s of deoxyHb-RBCs obtained from SCD patients can be also observed in Fig. 3, where the comparison between the groups of samples is performed for each chemical treatment. Especially, Fig. 3 b) reports a decreased u_s of deoxyHb-RBCs for the TP and NTP samples in comparison to HD. When comparing u_m for the three different groups (Figs. 3 a)-c)), it can be seen that SCD samples (especially the TP) report the highest values, also presented in Table I. In fact, the largest difference in u_m between HD and SCD samples is found when comparing oxyHb-RBCs from HD and TP. Seen in Table I, the average oxyHb-RBC u_m values for HD and TP are −0.33 and −0.14 μm/s, respectively. The high magnetic velocity of oxyHb-RBCs from TP samples suggests that the RBCs from these patients have impaired oxygen binding capabilities (i.e., they are not fully oxygenated). It may also suggest the effect of a slightly higher magnetization of Fe in the oxygenated HbS molecule compared to that in the HbA molecule, as reported by quantum-mechanical simulations [30]. As seen in Fig. 3 a), oxygenated TP samples also have a significant fraction of cells with a u_m above 0.

Fig. 4 reports the estimated MCH and MCHC values for HD, NTP, and TP samples when using the CTV data obtained from deoxyHb-RBCs and metHb-RBCs. First, it can be seen

that for both parameters, the values obtained when using deoxyHb-RBCs are higher than that of metHb-RBCs. This suggests the possible formation of hemichrome when converting oxyHb into metHb. This may be due to over-oxidation with sodium nitrite, which further oxidizes metHb into hemichrome, where the Fe atom no longer has five free electrons, but instead forms a covalent bond with a neighboring histidine ring and thus, results in a diamagnetic form of Hb. DeoxyHb, on the other hand, oxidizes into metHb if treated with excess sodium dithionite. Because the susceptibilities of the two Hb forms are paramagnetic and similar in magnitude, the possibility of side reactions is ignored for deoxyHb-RBCs.

Second, the average MCH and MCHC for HD samples are lower than that of SCD samples. This is speculated to be attributed to the different intracellular Fe content, cell size/volume, shape, and density of sickle RBCs. It has been suggested in the literature that dehydrated, hyperdense RBCs with high MCHC values are a distinguishing feature of SCD [42]. These cells are believed to play an important role in the pathogenesis of the disease, due to their increased propensity to undergo polymerization and sickling. However, the fraction of hyperchromic RBCs present in the blood of SCD patients may vary according to clinical conditions, especially before or during acute painful crises [26].

Third, it can be observed from the plots (where the normal range for MCH and MCHC is represented by a dashed rectangle) that although the MCH values are close to the normal levels (30 pg/cell) for the three groups of samples, the MCHC values are below the normal range [43]. This is attributed to the difference in estimating the RBC volume or mean corpuscular volume (MCV) using CTV data. We have previously published that even though the MCV obtained from CTV and the Coulter Counter are comparable for healthy RBCs [17], these values are lower than the normal MCV reference range for healthy donors (80–100 fL) [43].

B. RBC Size Distribution

Table I reports the average RBC size for each individual sample and Fig. 5 a) presents a histogram representing the cell diameter for the combined HD, TP, and NTP sample types, measured by the Coulter Counter. It can be seen from Table I that the average RBC sizes for both healthy donors and SCD patients are similar. Surprisingly, the average diameter for HD and TP is identical (4.64 ± 0.44 and 4.64 ± 0.49 μm, respectively), which is slightly less than that of SCD patients who did not receive a transfusion (4.73 ± 0.49 μm). The larger standard deviations for TP and NTP samples are equal further demonstrated by the tall peak of the HD histogram when overlaying the RBC diameter distributions for the combined three different donor types presented in Fig. 5 a). The peak diameters are quite close, but the NTP curve is right-shifted. The fraction of NTP RBCs with diameters greater than 5 μm is higher than that of TP and HD. This suggests that larger erythrocytes exist among those with SCD and that transfusion of healthy, monodisperse RBCs dilute these large cells after exchange transfusion. These large cells may be reticulocytes which have greater presence in SCD patients, particularly in the early stages of crisis. [43–45] Fig. 5 b) presents histograms of u_s data for metHb-RBCs for the three types of donors. In this case, a small right-shift is observed for TP samples compared to HD and a further right-shift is observed for NTP samples compared to TP. The significance between these findings can be explained

with (2). While the size histogram suggests the presence of large cells in NTP, studying the sedimentation curve suggests that size, density, drag, or a combination of all three, are responsible for the difference. Similarly, NTP samples have the fastest sedimentation, followed by the sickled and healthy mixture in TP samples. Although reticulocyte density is smaller in healthy, HbSS and sickle cell anemia cases, reticulocytes are denser than the rest of RBCs for HbSC. We believe the increased sedimentation is due to increased density in mature SCD erythrocytes.

C. BOBS Results

Since a "right shift" in an O_2 binding curve plot is a well-known characteristic of SCD, and as presented above, and previously published, the degree to which a RBC has bound O_2 significantly affects the magnetic susceptibility of RBCs, we used a BOBS to analyze the ability of sickle RBCs to bind O_2 as well as to estimate the magnetic properties of SCD patients' blood under intermediate oxygen levels. Fig. 6 presents overlaid O_2 equilibrium curves that plot the % saturation of O_2 in the erythrocyte Hb as a function of pO_2 for HD, TP and NTP. The data show that the P_{50} of HD and TP RBCs are quite similar (see Table I), with a slightly lower P_{50} for HD than TP, while the P_{50} and overall O_2 affinity for NTP are higher and lower, respectively, compared to HD RBCs. This result with the TP donor samples could be attributed to the mixture of healthy and SCD RBCs contained in the apheresis product sample (TP), in comparison to the only native, HbS-containing RBCs of NTP samples. In fact, Table I reveals that the P_{50} of HD and TP RBCs are very close and are within the healthy range (30–32 mmHg). However, this observation comes from a curve that represents many individual oxygen equilibrium curves and the inherent biological variance should not be forgotten. It is noted that the BOBS software fits the raw data to the Hill equation and then reports the P_{50} value based on the fit.

The shape of the NTP samples curve suggests decreased cooperativity compared to the other samples. O_2 saturation increases linearly with pO_2 below 20 mmHg, rather than a sigmoidal relationship, where O_2 rapidly binds to Hb due to cooperative changes in structure when Hb enters the R state [4]. It has been reported that NTP samples have higher amounts of HbS as well as higher HbF compared to HD and TP samples [28]. The two species have opposing effects on O_2 affinity; more HbS increases the concentration of $\alpha_2\beta^{S}{}_2$ tetramers and therefore Hb in the T state, which are sensitive to polymerization. However, increased HbF yields more benign $\alpha_2\beta^{S}\gamma$ and $\alpha_2\gamma_2$ tetramers upon dimer dissociation and reassociation, resulting in less sickling. Additionally, high amounts of HbF result in larger cell volume, further decreasing MCHC and increasing the "delay time" of sickling, contributing to sickling reduction. Although native HbF is removed during RBC exchange apheresis, it appears that SCD patients benefit from higher oxygen affinity due to diminished HbS after receiving an exchange transfusion [28].

In many cases for TP and NTP samples, overlaid raw and fitted data reveal that the Hill fit overestimates Hb O_2 saturation, particularly in the 0–20 mmHg region of the oxygen equilibrium curve. This results in a small underestimation of P_{50} and a severe overestimation of cooperativity (n). Therefore, the Adair model is chosen to describe O_2

binding equilibria moving forward, and also to estimate the magnetic moment of the samples under intermediate pO_2 values.

Combining O_2 saturation data and the Adair model parameters allows us to calculate the magnetic character of the samples, after determining the equilibrium constants K_i for intracellular Hb bound to "i" number of oxygen atoms (where $1 \leq i \leq 4$). The results are presented in Fig. 7, where the magnetic moment of the samples as a function of pO_2 is presented for the five HD, NTP and TP samples. The data reveal substantial changes in the Hb's magnetic moment of the RBCs (as much as a factor of 2.5) between HD and NTP samples at intermediate pO_2. This is attributed to the low O_2 % saturation of TP samples in the pO_2 range of 20–100 mmHg, as seen in Fig. 6. The higher magnetic moment of the NTP samples oxygenated by the room air (at pO2 = 150 mmHg) compared to the HD and NTP samples is also consistent with the reported differences between O_2-HbS and O_2-HbA Fe magnetizations by quantum-mechanical simulations [30].

While clinical metrics such as MCH and MCHC are extremely useful in diagnosis and treatment, the small differences in average Hb between donors and modest variation within a donor require extremely high resolution and selectivity in detection/separation technology. Exploiting this additional condition, pO_2, on a heterogeneous mixture of healthy and HbS-containing cells can potentially lead to higher accuracy and efficiency in detecting and separating sickle RBCs than simply targeting the quantity of Hb alone. Furthermore, the scatter plots in Figs. 3 a) and 3 b) suggest that cells with higher u_m (analogous to MCH) also have higher u_s (analogous to size, assuming density and drag are constant) under fully deoxygenated conditions. This leads to an unfortunate fact; the larger cells that are prone to sickling and vaso-occlusion could be misidentified as healthy cells with abundant Hb. At an intermediate pO_2, the large, Hb-rich RBCs with low concentrations of HbS that sits in the upper-right quadrant of the scatter plots in Figs. 3 a) and b) will shift to the left, due to higher oxygen affinity and therefore lower magnetic moment/susceptibility.

In a similar approach to this paper with respect to analyzing single RBC from healthy and SCD patients, Di Caprio et al (2019) [46] have also reported on a microfluidic device that determines the oxygen saturation of each RBC on at a time using spectroscopic measurements. They report that not only is there a difference in oxygen saturation between SCD and normal RBCs, but that this difference is more apparent, and bimodal in partial saturation conditions. Since only healthy and transfusion discarded blood (TP in this current study) was used, it is not known whether this bimodal distribution of the oxygen saturation data is the result of this mixed blood sample (healthy and SCD RBCs), or if a bimodal distribution is apparent in pure SCD RBCs.

IV. Conclusions

In this study, we report the magnetic characteristics of SCD RBCs and explore the potential of magnetophoresis for diagnosis, quantification of sickle RBCs, and separation of sickle from healthy RBCs for patients receiving exchange transfusions. Such a device would reduce the demand of RBC units and avoid adverse effects from transfusions. However,

information about the entire population of SCD RBCs at the single cell level is needed. Thus, we compared RBCs from SCD patients with and without transfusions to RBCs from healthy donors.

Our experiments reveal a small sub-population of large SCD cells, confirming the presence of elongated, irreversibly sickled RBCs. Additionally, CTV quantified the response to magnetic and gravitational fields under several chemical states. Interestingly, SCD deoxyHb-RBCs reported decreased u_s, suggesting decreased density, decreased size, or increased drag due to a shape change when treated with sodium dithionite while this was not observed for HD samples. The average MCH and MCHC for HD samples is lower than SCD samples, suggesting dehydrated hyperdense RBCs with high MCHC in SCD blood. The high u_m of oxyHb-RBCs from TP samples is attributed to impaired O_2 binding capabilities of sickle RBCs (i.e., not fully oxygenated when in contact with O_2).

Oxygen-Hb equilibrium curves paired with magnetic and kinetic data led to the estimation of magnetic characteristics of SCD cells under intermediate oxygenation. Our results confirm decreased O_2 affinity of sickle RBCs (especially for NTP). Moreover, calculated magnetic moments at intermediate pO_2 suggest NTP samples have the highest magnetic moments (around twice that of TP and HD samples at particular pO_2). This could be attributed to a mixture of healthy and native RBCs contained in the apheresis sample (TP). These data may lead to developing a rapid and affordable device to diagnose and selectively remove sickle cells from patients undergoing transfusions.

Acknowledgment

The authors thank Dr. Eduardo Reátegui and Nicole Walters for drawing healthy donor blood samples on their IRB (2018H0268).

This work is supported by the National Heart, Lung, and Blood Institute (1R01HL131720-01A1) and DARPA (BAA07-21).

References

Basic format for books:

[1]. “Join the fight against sickle cell disease,” American Red Cross. [Online]. Available: https://www.redcrossblood.org/donate-blood/bloodtypes/diversity/sicklecell.html. [Accessed: 12-Jan-2022].

[2]. Ware RE et al. , “Sickle cell disease,” Lancet, vol. 390, no. 10091, pp. 311–323, 2017, doi: 10.1016/S0140-6736(17)30193-9. [PubMed: 28159390]

[3]. Knowlton SM et al. , “Sickle cell detection using a smartphone,” Sci. Rep, vol. 5, pp. 1–11, 2015, doi: 10.1038/srep15022.

[4]. Eaton WA et al. , “Is cooperative oxygen binding by hemoglobin really understood?” Rend. Lincei, vol. 17, no. 1–2, pp. 147–162, 2006, doi: 10.1007/BF02904506.

[5]. “Sickle cell trait,” American Society of Hematology. [Online]. Available: https://www.hematology.org/education/patients/anemia/sickle-cell-trait. [Accessed: 12-Jan-2022].

[6]. Agrawal RK et al. , “Hydroxyurea in sickle cell disease: drug review,” Indian J. Hematol. Blood Transfus, vol. 30, no. 2, pp. 91–96, 2014, doi: 10.1007/s12288-013-0261-4. [PubMed: 24839362]

[7]. Muteb PB et al. , “Efficacy, tolerability and cost of partial transfusion exchanges in sickle cell disease in a sickle cell syndrome management centre in sub-Saharan Africa,” Medecine et Sante Tropicales, vol. 27, no. 4, pp. 387–391, 2017, doi: 10.1684/mst.2017.0719. [PubMed: 29313505]

[8]. Chou ST et al. , “American society of hematology 2020 guidelines for sickle cell disease: transfusion support,” Blood Adv., vol. 4, no. 2, pp. 327–355, 2020, doi: 10.1182/BLOODADVANCES.2019001143. [PubMed: 31985807]

[9]. Stussi G. et al. , “Red blood cells: exchange, transfuse, or deplete,” Transfus. Med. Hemotherapy, vol. 46, no. 6, pp. 407–416, 2019, doi: 10.1159/000504144.

[10]. Stevens M. et al. , “The British Childhood Cancer Survivor Study: objectives, methods, population structure, response rates and initial descriptive information,” Pediatr. Blood Cancer, vol. 50, no. 5, pp. 1018–1025, 2008, doi: 10.1002/pbc. [PubMed: 17849473]

[11]. Steele C. et al. , “Point-of-care screening for sickle cell disease in low-resource settings: a multi-center evaluation of HemoTypeSC, a novel rapid test,” Am. J. Hematol, vol. 94, no. 1, pp. 39–45, 2019, doi: 10.1002/ajh.25305. [PubMed: 30290004]

[12]. Arishi WA, Al-hadrami HA, and Zourob M, “Techniques for the detection of sickle cell disease: A review,” Micromachines, vol. 12, no. 5, pp. 1–22, 2021, doi: 10.3390/mi12050519.

[13]. Pauling L. and Coryell CD, “The magnetic properties and structure of the hemochromogens and related substances,” PNAS, vol. 22, pp. 159–163, 1936, doi: 10.1073/pnas.22.3.159. [PubMed: 16588065]

[14]. Pauling L. and Coryell CD, “The magnetic properties and structure of the hemoglobin, oxyhemoglobin and carbonmonoxyhemoglobin,” PNAS, vol. 22, pp. 210–216, 1936, doi: 10.1073/pnas.22.4.210. [PubMed: 16577697]

[15]. Zborowski M. et al. , “Red blood cell magnetophoresis,” Biophys. J, vol. 84, no. 4, pp. 2638–2645, 2003, doi: 10.1016/S0006-3495(03)75069–3. [PubMed: 12668472]

[16]. Melville D. et al. , “Direct magnetic separation of red cells from whole blood,” Nature, vol. 255, no. 5511, pp. 706, 1975, doi: 10.1038/255706a0. [PubMed: 1134566]

[17]. Gómez-Pastora J. et al. , “Analysis of separators for magnetic beads recovery: from large systems to multifunctional microdevices,” Sep. Purif. Technol, vol. 172, pp. 16–31, 2017, doi: 10.1016/j.seppur.2016.07.050.

[18]. Kim J. et al. , “Quantification of the mean and distribution of hemoglobin content in normal human blood using cell tracking velocimetry,” Anal. Chem, vol. 92, no. 2, pp. 1956–1962, 2020, doi: 10.1021/acs.analchem.9b04302. [PubMed: 31874030]

[19]. Kim J. et al. , “A subpopulation of monocytes in normal human blood has significant magnetic susceptibility: quantification and potential implications,” Cytom. Part A, vol. 95, no. 5, pp. 478–487, 2019, doi: 10.1002/cyto.a.23755.

[20]. Furlani EP, “Magnetophoretic separation of blood cells at the microscale,” J. Phys. D. Appl. Phys, vol. 40, no. 5, pp. 1313–1319, 2007, doi: 10.1088/0022-3727/40/5/001.

[21]. Knowlton SM et al. , “Magnetic levitation coupled with portable imaging and analysis for disease diagnostics,” J. Vis. Exp, vol. 2017, no. 120, pp. 1–9, 2017, doi: 10.3791/55012.

[22]. Thompson L. et al. , “Quantification of cellular densities and antigenic properties using magnetic levitation,” JOVE, vol. 171, 2021, doi: 10.3791/62550.

[23]. Baday M. et al. , “Integrating cell phone imaging with magnetic levitation (i-LEV) for label-free blood analysis at the point-of-living,” Small, vol. 12, no. 9, pp. 1222–1229, 2016, doi: 10.1002/smll.201501845. [PubMed: 26523938]

[24]. Kumar AA et al. , “Density-based separation in multiphase systems provides a simple method to identify sickle cell disease,” PNAS, vol. 111, no. 41, pp. 14864–14869, 2014, doi: 10.1073/pnas.1414739111. [PubMed: 25197072]

[25]. Ge S. et al. , “Magnetic levitation in chemistry, materials science, and biochemistry,” Angew. Chemie - Int. Ed, vol. 59, no. 41, pp. 17810–17855, 2020, doi: 10.1002/anie.201903391.

[26]. Maruyama T. et al. , “Physiological and pathophysiological significance of erythrocyte senescence, density and deformability: important but unnoticed trinity,” J. Biorheol, vol. 34, no. 2, pp. 61–70, 2020, doi: 10.17106/jbr.34.61.

[27]. Brugnara C. and Mohandas N, “Red cell indices in classification and treatment of anemias: from M.M. Wintrobes’s original 1934 classification to the third millennium,” Curr. Opin. Hematol, vol. 20, no. 3, pp. 222–230, 2013, doi: 10.1097/MOH.0b013e32835f5933. [PubMed: 23449069]

[28]. Seakins M. et al. , “Erythrocyte Hb-S concentration. An important factor in the low oxygen affinity of blood in sickle cell anemia,” J. Clin. Invest, vol. 52, no. 2, pp. 422–432, 1973, doi: 10.1172/JCI107199. [PubMed: 4683881]

[29]. Eaton WA and Bunn HF, “Treating sickle cell disease by targeting HbS polymerization,” Blood, vol. 129, no. 20, pp. 2719–2726, 2017, doi: 10.1182/blood-2017-02-765891. [PubMed: 28385699]

[30]. Eldeniz C. et al. , “Bulk volume susceptibility difference between deoxyhemoglobin and oxyhemoglobin for HbA and HbS: a comparative study,” Magn. Reson. Med, vol. 85, no. 6, pp. 3383–3393, 2021, doi: 10.1002/mrm.28668. [PubMed: 33475200]

[31]. Novoselov DY, Korotin DM, and Anisimov VI, “Features of the electronic structure of the active center of an HbS molecule,” Russ. J. Phys. Chem A, vol. 90, no. 1, pp. 113–116, 2016, doi: 10.1134/S0036024416010209.

[32]. Mayda S. et al. , “Magnetic mechanism for the biological functioning of hemoglobin,” Sci. Rep, vol. 10, no. 1, pp. 1–7, 2020, doi: 10.1038/s41598-020-64364-y. [PubMed: 31913322]

[33]. Gómez-Pastora J. et al. , “Intrinsically magnetic susceptibility in human blood and its potential impact on cell separation: non-classical and intermediate monocytes have the strongest magnetic behavior in fresh human blood,” Exp. Hematol, vol. 99, pp. 21–31, 2021, doi: 10.1016/j.exphem.2021.05.003. [PubMed: 34015390]

[34]. Weigand MRH et al. , “Magnetophoretic and spectral characterization of oxyhemoglobin and deoxyhemoglobin: chemical versus enzymatic processes,” PLoS One, vol. 16, no. 9, pp. 1–14, 2021, doi: 10.1371/journal.pone.0257061.

[35]. Chalmers JJ et al. , “Femtogram resolution of iron content on a per cell basis: ex vivo storage of human red blood cells leads to loss of hemoglobin,” Anal. Chem, vol. 89, no. 6, pp. 3702–3709, 2017, doi: 10.1021/acs.analchem.7b00007. [PubMed: 28230974]

[36]. Xue W. et al. , “Single cell magnetometry by magnetophoresis vs. bulk cell suspension magnetometry by SQUID-MPMS – a comparison,” J. Magn. Magn. Mater, vol. 474, pp. 152–160, 2019, doi: 10.1016/j.jmmm.2018.10.108. [PubMed: 32863537]

[37]. Kim J. et al. , “Single cell analysis of aged RBCs: quantitative analysis of the aged cells and byproducts,” Analyst, vol. 144, no. 3, pp. 935–942, 2019, doi: 10.1039/c8an01904e. [PubMed: 30617361]

[38]. Zhbanov A. and Yang S, “Effects of aggregation on blood sedimentation and conductivity,” PLoS One, vol. 10, no. 6, pp. 1–25, 2015, doi: 10.1371/journal.pone.0129337.

[39]. Tinevez JY et al. , “TrackMate: an open and extensible platform for single-particle tracking,” Methods, vol. 115, pp. 80–90, 2017, doi: 10.1016/j.ymeth.2016.09.016. [PubMed: 27713081]

[40]. Hill AV, “The possible effects of the aggregation of the molecules of hæmoglobin on its dissociation curves,” J. Physiol, vol. 40, pp. 4–7, 1910, doi: 10.1113/jphysiol.1910.sp001386.

[41]. Scrima R. et al. , “Hemoglobin non-equilibrium oxygen dissociation curve,” bioRxiv, 2019, doi: 10.1101/2020.01.09.900001.

[42]. Smith NA, “Measurement of red blood cell oxygenation state by magnetophoresis,” M.S. thesis, Dept. Chem. Biomed. Eng, Cle. St. Univ., Cleveland, OH, 2019.

[43]. Brugnara C, “Reticulocyte cellular indices: a new approach in the diagnosis of anemias and monitoring of erythropoietic function,” Crit. Rev. Clin. Lab. Sci, vol. 37, no. 2, pp. 93–130, 2000, doi: 10.1080/10408360091174196. [PubMed: 10811141]

[44]. Stuart MJ and Nagel RL, “Sickle-cell disease,” Lancet, vol. 364, no. 9442, pp. 1343–1360, 2004, doi: 10.1016/S0140-6736(04)17192-4. [PubMed: 15474138]

[45]. Ballas SK and Smith ED, “Red blood cell changes during the evolution of the sickle cell painful crisis,” Blood, vol. 79, no. 8, pp. 2154–2163, 1992, doi: 10.1182/blood.v79.8.2154.bloodjournal7982154. [PubMed: 1562742]

[46]. Di Caprio G. et al. High-throughput assessment of hemoglobin polymer in single red blood cells from sickle cell patients under controlled oxygen tension. PNAS, vol. 116, no. 50, pp. 25236–25242, 2019. [PubMed: 31767751]

[47]. Piety NZ, Gifford SC, Yang X, and Shevkoplyas SS, “Quantifying morphological heterogeneity: A study of more than 1 000 000 individual stored red blood cells,” Vox Sang., vol. 109, no. 3, pp. 221–230, 2015, doi: 10.1111/vox.12277. [PubMed: 25900518]

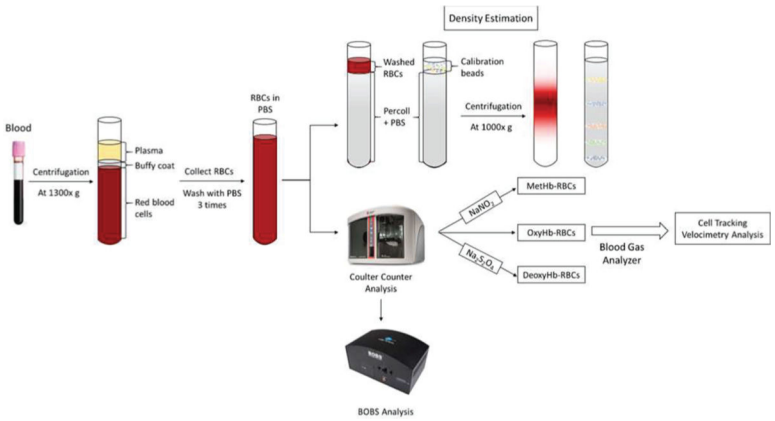

Fig. 1.

Sample preparation procedure scheme. First, RBCs from whole blood samples (for HD and NTP samples) were collected by centrifugation. All RBC samples (from HD, TP and NTP) were washed three times with PBS. The density of the samples was estimated using a Percoll gradient and density marker beads. The washed RBCs were analyzed using Coulter Counter (size/concentration distribution) and BOBS (for determining the oxygen-Hb equilibrium curve). For CTV analysis, oxyHb-RBCs were processed directly, and metHb-RBCs and deoxyHb-RBCs were obtained by treating the RBCs with $NaNO_2$ and $Na_2S_2O_4$, respectively. The same protocol was applied on all blood samples, which were processed the same day of blood draw.

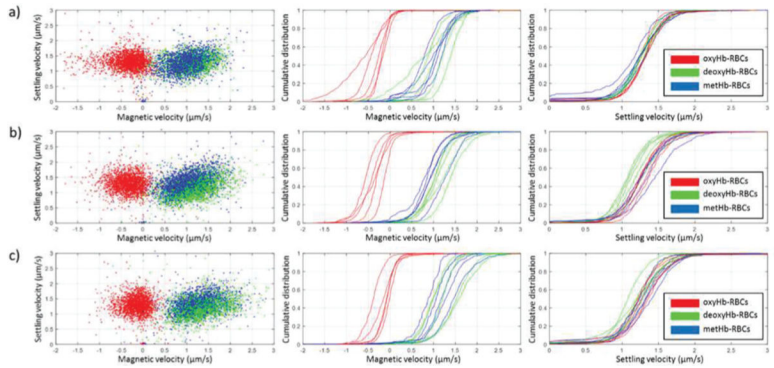

Fig. 2.

Scatter plot and cumulative distribution curves of u_m and u_s for oxyHb-RBCs (red), deoxyHb-RBCs (green) and metHb-RBCs (blue) for a) HD, b) NTP and c) TP samples presented in Table I. The dot plot shows u_m and u_s values of individual RBCs (left panel), whereas the central and right panels present the u_m and u_s cumulative distribution curves for each donor/patient, respectively.

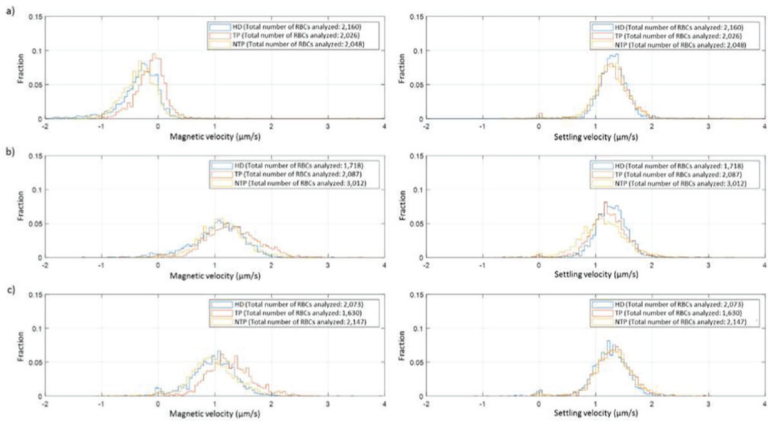

Fig. 3.

Histograms of magnetic (left) and settling (right) velocities for a) oxyHb-RBCs, b) deoxyHb-RBCs and c) metHb-RBCs. The data contained on each panel combines all the RBCs for each group of samples (i.e., HD, TP and NTP).

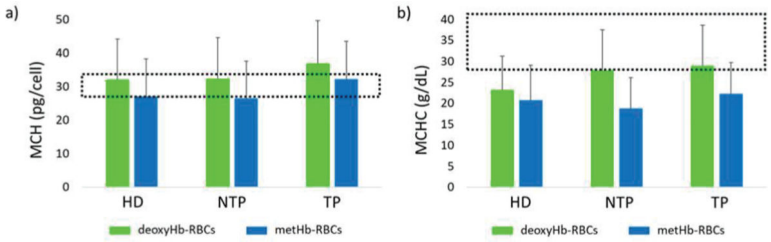

Fig. 4.

Average a) MCH and b) MCHC values for HD, NTP and TP samples when both the deoxyHb-RBC and the metHb-RBC data are employed for the calculations. The normal range for MCH (27–33 pg/cell) and for MCHC (28–41 g/dL) are represented by the dashed rectangle.

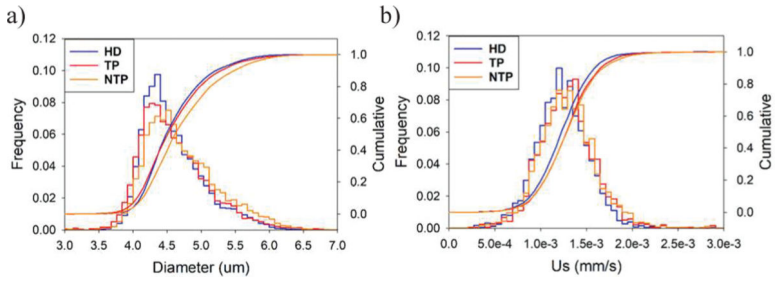

Fig. 5.

a) Histograms of the RBC diameter measured on Coulter Counter and grouped for HD (blue), TP (red) and NTP (orange) samples. The histograms closely overlay and there is a very little difference in cell diameter between the RBC sources. b) MetHb-RBC settling velocity, which is proportional to cell diameter squared, for HD (blue), TP (red) and NTP (orange) donors. The slight right-shift in u_s suggests a difference in cell density between healthy and SCD patients, as presented in Table I.

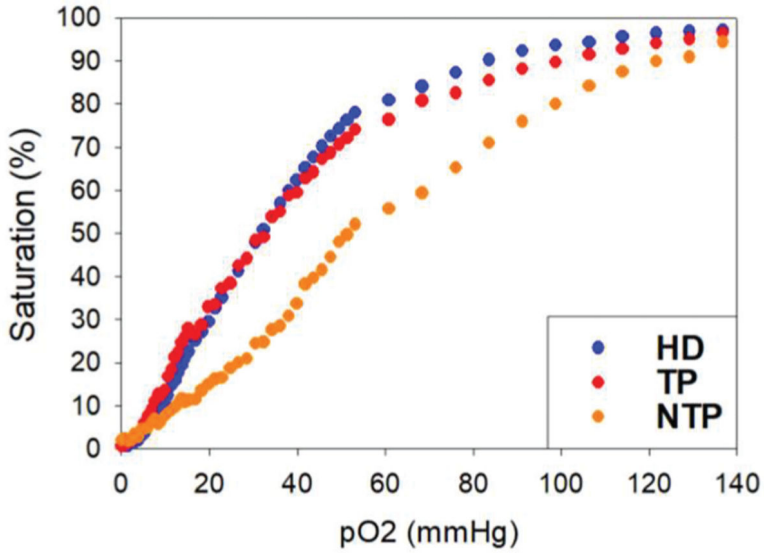

Fig. 6.
Oxygen equilibrium curves for HD (blue), TP (red) and NTP (orange).

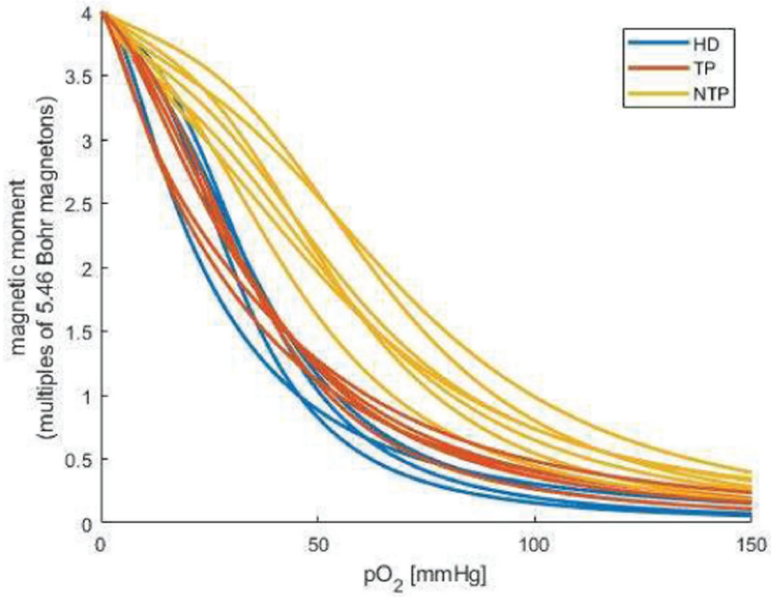

Fig. 7.

Magnetic moment of HD (blue), TP (red), and NTP (orange) RBC samples as a function of pO2. The lower oxygenation affinity of NTP samples in comparison to HD and TP results in a lower saturation, and therefore higher magnetic moments under intermediate oxygen levels.

TABLE I

N, AND IRON DATA OF HEALTHY AND SCD RBCS WITH DEOXYGENATED AND OXIDIZED HEMOGLOBIN

(μm)	Us_{oxyHb}(μm/s)	Um_{oxyHb}(μm/s)	$Us_{deoxyHb}$(μm/s)	$Um_{deoxyHb}$(μm/s)	Us_{metHb}(μm/s)	Um_{metHb}(μm/s)	$MCH_{deoxyHb}$(pg)	$MCHC_{deoxyHb}$(g/dL)	MCH_{metHb}(pg)	$MCHC_{metHb}$(g/dL)	P_{50}(mmHg)
4.66 0.43	1.30 ±0.31	−0.65 ± 0.53	1.28 ±0.33	0.77 ± 0.63	1.24 ±0.34	0.95 ±0.51	24.6 ± 16.4	19.0 ± 12.6	25.4 ± 12.9	20.7 ± 10.1	33.1
4.61 0.43	1.30 ±0.25	−0.17 ±0.21	1.21 ±0.48	1.07 ±0.41	1.24 ±0.39	1.15 ±0.37	31.6 ± 12.0	22.6 ±6.95	31.5 ± 11.8	22.7 ±7.38	30.9
4.61 0.45	1.21 ±0.43	−0.17 ±0.34	1.24 ±0.26	1.38 ±0.29	1.07 ± 0.46	1.04 ±0.43	42.5 ± 11.0	27.8 ±5.53	28.3 ± 13.1	21.8 ±9.02	23.5
.66 ± 0.45	1.31 ±0.27	−0.40 ±0.57	1.30 ±0.30	0.86 ±0.36	1.24 ±0.33	0.78 ± 0.34	25.5 ± 10.8	19.3 ±8.13	20.6 ±9.93	16.7 ±7.73	32.9
.68 ± 0.42	1.34 ±0.29	−0.27 ±0.26	1.28 ±0.28	1.21 ±0.30	1.31 ±0.34	1.05 ±0.31	35.7 ± 10.6	27.3 ±6.85	28.3 ±9.50	21.4 ± 7.96	33.0
.64 ± 0.44	1.29 ±0.31	−0.33 ±0.38	1.26 ±0.33	1.06 ± 0.40	1.22 ±0.37	1.00 ± 0.39	32.0 ± 12.2	23.2 ±8.02	26.8 ± 11.4	20.7 ±8.43	30.7
4.74 0.50	1.24 ± 0.29	−0.35 ± 0.52	1.20 ±0.29	1.18 ± 0.48	1.26 ±0.36	0.76 ±0.41	32.3 ± 14.0	31.0 ± 12.8	19.9 ± 10.4	17.9 ±8.87	60.7
.73 ± 0.46	1.39 ±0.32	−0.57 ±0.26	1.29 ±0.33	1.42 ±0.38	1.45 ±0.36	1.27 ±0.37	42.4 ± 14.1	30.2 ±8.17	36.4 ± 12.8	21.9 ± 7.09	40.6
.79 ± 0.45	1.32 ±0.28	−0.11 ±0.22	1.12 ±0.36	1.02 ± 0.74	1.35 ±0.43	0.84 ±0.36	27.0 ± 10.1	26.9 ±9.96	23.0 ±9.76	17.3 ±6.05	47.2
.63 ± 0.50	1.24 ±0.28	−0.30 ±0.23	1.07 ±0.29	1.08 ±0.37	1.25 ±0.34	0.95 ± 0.40	32.1 ± 12.1	24.2 ±8.20	27.6 ± 12.1	16.7 ±7.53	52.0
.78 ± 0.55	1.28 ±0.31	−0.42 ± 0.29	1.10 ±0.29	1.01 ±0.34	1.25 ±0.33	0.97 ±0.86	27.6 ± 10.8	26.8 ±9.14	24.8 ± 11.1	19.3 ±7.72	61.1
.73 ± 0.49	1.29 ±0.29	−0.35 ±0.30	1.16 ±0.31	1.14 ±0.46	1.31 ±0.36	0.96 ± 0.48	32.3 ± 12.2	27.8 ±9.66	26.3 ± 11.2	18.6 ±7.5	52.3
4.71 0.51	1.36 ±0.36	−0.09 ± 0.22	1.29 ±0.38	1.50 ± 0.42	1.32 ±0.35	1.48 ± 0.47	43.3 ± 14.5	35.8 ± 10.9	39.0 ± 13.0	30.7 ± 10.9	31.4
4.72 0.52	1.34 ±0.39	−0.08 ± 0.20	1.26 ±0.36	1.58 ± 0.48	1.38 ±0.42	1.26 ±0.39	44.9 ± 16.1	37.6 ± 11.0	34.0 ± 12.6	24.8 ± 7.72	24.9
4.51 0.44	1.34 ±0.61	−0.12 ±0.73	1.22 ±0.32	0.99 ± 0.44	1.22 ± 0.40	1.15 ±0.46	30.5 ± 10.2	19.7 ± 7.73	33.4 ± 12.1	20.5 ±6.97	32.2
4.67 0.52	1.19 ±0.40	−0.01 ±0.22	1.19 ±0.41	1.02 ±0.36	1.34 ±0.47	1.05 ±0.32	31.7 ± 13.9	21.9 ± 11.1	31.4 ± 10.4	17.1 ±4.67	27.6
4.57 0.46	1.24 ±0.26	−0.39 ± 0.24	1.09 ±0.26	1.19 ±0.28	1.21 ±0.30	0.86 ±0.28	33.2 ±9.53	29.6 ± 7.40	22.7 ±8.32	17.6 ± 7.38	31.9

IEEE Trans Biomed Eng. Author manuscript; available in PMC 2023 December 01.

US_{oxyHb}(μm/s)	Um_{oxyHb}(μm/s)	$US_{deoxyHb}$(μm/s)	$Um_{deoxyHb}$(μm/s)	US_{metHb}(μm/s)	Um_{metHb}(μm/s)	$MCH_{deoxyHb}$(pg)	$MCHC_{deoxyHb}$(g/dL)	MCH_{metHb}(pg)	$MCHC_{metHb}$(g/dL)	P_{50}(mmHg)
1.29 ± 0.40	−0.14 ±0.32	1.21 ±0.34	1.25 ±0.39	1.29 ±0.39	1.16 ±0.38	36.7 ± 12.8	28.9 ±9.63	32.1 ± 11.3	22.1 ± 7.52	29.6